Calatayud, J.; Cortés, J.; Jornet, M. (2020). Computing the density function of complex models with randomness by using polynomial expansions and the RVT technique. Application to the SIR epidemic model. Chaos, Solitons and Fractals. 133:1-10. https://doi.org/10.1016/j.chaos.2020.109639

Computing the density function of complex models with randomness by using polynomial expansions and the RVT technique. Application to the SIR epidemic model

Julia Calatayud[a], Juan Carlos Cortés[a], Marc Jornet[a,*]

[a]*Instituto Universitario de Matemática Multidisciplinar,*
Universitat Politècnica de València,
Camino de Vera s/n, 46022, Valencia, Spain

Abstract

This paper concerns the computation of the probability density function of the stochastic solution to general complex systems with uncertainties formulated via random differential equations. In the existing literature, the uncertainty quantification for random differential equations is based on the approximation of statistical moments by simulation or spectral methods, or on the computation of the exact density function via the random variable transformation (RVT) method when a closed-form solution is available. However, the problem of approximating the density function in a general setting has not been published yet. In this paper, we propose a hybrid method based on stochastic polynomial expansions, the RVT technique, and multidimensional integration schemes, to obtain accurate approximations to the solution density function. A problem-independent algorithm is proposed. The algorithm is tested on the SIR (susceptible-infected-recovered) epidemiological model, showing significant improvements compared to the previous literature.

Keywords: complex model with uncertainties, random differential equation, probability density function, stochastic polynomial expansion, RVT technique, SIR epidemic model
2010 MSC: 34F05, 60H10, 60H35, 65C30, 92D30

1. Introduction

This paper is concerned with complex systems with uncertainties formulated via random differential equations, whose parameters are random variables having any type of probability distributions [1, 2, 3, 4].

Several methods have been proposed in the literature to obtain statistical information of the stochastic solution to random differential equations (uncertainty quantification). Monte Carlo simulation is a popular statistical method based on obtaining realizations of the solution, which allows approximating its statistical moments from the generated sample [5]. Although it is a

*Corresponding author
Email addresses: jucagre@doctor.upv.es (Julia Calatayud), jccortes@imm.upv.es (Juan Carlos Cortés), marjorsa@doctor.upv.es (Marc Jornet)

robust and easy to implement approach, this technique may become inefficient due to the slow convergence rate. Thus, more research has been devoted to non-statistical methods, where instead of employing realizations, the goal is different, specifically reconstructing the functional dependence of the solution on the input parameters. The perturbation method [6], the differential transform technique [7], and homotopy methods [8, 9] have been applied to different kinds of models. A fruitful approach for the study of models with uncertainties consists in using spectral expansions of the solution in terms of the random inputs. Polynomial chaos (PC) methods expand stochastic quantities in terms of Hermite polynomials when there is functional dependence on independent Gaussian parameters [10]. This method was extended to generalized polynomial chaos (gPC) expansions, to alleviate the difficulties arising in non-Gaussian problems [11, 12]. The optimal polynomial basis is selected depending on the probability distribution of the parameters. If the parameters are independent and their distributions belong to the Askey scheme, the corresponding family of orthogonal polynomials is selected (for instance, Legendre polynomials are associated to the Uniform distribution). For any other probability distribution that does not readily dispose of an orthogonal family of polynomials, a numerical Gram-Schmidt orthogonalization procedure can be carried out [13, 14]. These expansions have spectral convergence in the mean square sense, when the moment problem for the random parameters is uniquely solvable [12, 15]. In the setting of random differential equations, the stochastic Galerkin projection technique uses truncated gPC expansions based on the random input parameters to approximate the solution. The Galerkin projections present rapid mean square convergence towards the solution [12, 16, 17, 18, 19]. When the inputs of the differential equation are not independent, polynomial expansions based on the canonical polynomial basis were proposed [20] (these are not gPC expansions). This method also presents fast mean square convergence, in general [21, 22], and compared to some orthogonal chaos bases (see [23, Section 2.3.3] or the Rosenblatt transformation in [12, Section 4.1.2]) it is easier to handle in computations.

The computation of the probability density function of specific random differential equations has been tackled recently using the random variable transformation (RVT) method [24, 25, 26, 27, 28]. This technique is feasible only when a simple closed-form solution exists. In other cases, one should use different representations of the solution, such as Karhunen-Loève expansions [29, 30], random power series [31] or finite difference numerical schemes [32, 33]. Recently, the authors of this paper with another colleague proposed a hybrid method combining gPC expansions and the RVT technique for stochastic models with one random input parameter [34]. We restricted to one degree of uncertainty because we were not able to apply the multidimensional version of the RVT technique to problems having more than one random parameter, as it was unclear for us how to derive the injectivity regions of multivariate polynomials. Sobol indices were utilized to select the random input parameter having the main effect on the output variance, and the rest of parameters were then set constant.

This paper supposes the complete extension of [34] to random differential equations with any degree of uncertainty. We combine polynomial expansions (in the independent and non-independent case of inputs), the RVT technique, and multidimensional integration schemes, to approximate fast and accurately the probability density function of the solution. An algorithm is proposed that is problem-independent.

Continuous models allow getting a better understanding of the global spread of epidemics [35, 36, 37]. Test-problems on the SIR (susceptible-infected-recovered) epidemic model are studied in this paper. The RVT technique alone has been utilized for SI and SIS-type epidemic models [38, 39]. However, since the SIR model does not present a simple closed-form solution to apply the RVT method, in contrast to the SI and SIS models, no faithful approximation of its

density function has been achieved. Accurate approximations of the expectation and the variance statistics of the SIR model solution were obtained in [40], by utilizing gPC expansions and the Galerkin projection technique. Only recently, the solution to the SIR model was approximated by linearizing differential equations, and the RVT method was then applied to derive a density function estimate [41]. Nonetheless, the approximated densities obtained in such way may differ significantly from the exact ones. In this paper, we will achieve fast and accurate approximations to the density function of the solution to the SIR model, as an application of our algorithm that combines polynomial expansions and the RVT technique.

2. Method to compute the density function of stochastic models

Consider a general random differential equation problem

$$\begin{cases} x'(t) = F(t, x(t), \eta), \ t \in I, \\ x(t_0) = x_0. \end{cases} \tag{1}$$

Here $I \subseteq \mathbb{R}$ is an interval containing t_0, F is a deterministic function, and the randomness arises from the random vector η and also maybe from components of the initial condition $x_0 = (x_{0,1}, \ldots, x_{0,q}) \in \mathbb{R}^q$. All the random variables from system (1) are supposed to be jointly absolutely continuous, but no independence is required. We let $\xi = (\xi_1, \ldots, \xi_s) \in \mathbb{R}^s$ be the random vector whose components are the random input parameters in (1) (subset of (η, x_0)), where $s < \infty$ is the uncertainty dimension. The density function of ξ_i is denoted as $f_{\xi_i}(\xi_i)$, and the joint density of ξ is $f_\xi(\xi)$. The term $x(t) = (x_1(t), \ldots, x_q(t))$ is a stochastic process $x : I \to \mathbb{R}^q$ that solves (1) (i.e. its trajectories solve the deterministic counterpart of (1) for any realization of ξ), having joint density function $f(x, t)$. We aim at computing the marginal density functions of $x_i(t)$, $f_i(x, t)$, for $i = 1, \ldots, q$.

If (1) has a closed-form solution, $x(t) = H(t, \xi)$ for certain deterministic function H, then the joint density $f(x, t)$ can be derived from the RVT method mentioned in Section 1. To do so, given $t \in I$, the transformation mapping $H(t, \cdot)$ should be injective with non-zero Jacobian J with respect to ξ, in an open partition $\{D_k\}_k$ of the support of ξ. In this case,

$$f(x, t) = \sum_{k:\, x \in H_k(D_k)} f_\xi(H_k^{-1}(t, x)) |J H_k^{-1}(t, x)|, \ x \in \mathbb{R},$$

where $H_k = H|_{D_k}$.

The problem arises when the solution to (1) is not known via a closed-form expression. To the best of our knowledge, no solution has been provided in the literature for this case in a general setting. We propose an algorithmic approach to approximate $f_i(x, t)$ based on stochastic polynomial expansions and the RVT method. We assume that each random input ξ_i has finite absolute moments of any order: $\mathbb{E}[|\xi_i|^r] < \infty$ for all $1 \leq r < \infty$, $1 \leq i \leq s$, where the operator $\mathbb{E}$ denotes the expectation. This condition will be necessary to assure that any polynomial evaluated at ξ_i has well-defined expectation, $1 \leq i \leq s$.

Suppose for the moment that $\xi_1, \ldots, \xi_s$ are independent random variables. Let $p \geq 1$. For $1 \leq i \leq s$, let $\{\phi_k^i(\xi_i)\}_{k=0}^\infty$ be a sequence of orthogonal polynomials (the degree of ϕ_k^i is k) with respect to the density $f_{\xi_i}(\xi_i)$. We are considering the weighted space $\mathrm{L}^2_{f_{\xi_i}}$ of real measurable functions h with finite norm $(\int_{\mathbb{R}} h(v)^2 f_{\xi_i}(v) \mathrm{d}v)^{1/2} < \infty$. When the distribution of ξ_i belongs to the Askey scheme, the family of polynomials is explicitly known (for instance, Hermite polynomials

correspond to Normal random variables, Legendre polynomials correspond to Uniform random variables, etc.) [12]. For any other distribution, a Gram-Schmidt orthogonalization procedure is carried out from the canonical basis $\{1, \xi_i, \xi_i^2, \xi_i^3, \ldots\}$ up to degree p [13, 14]. We define the s-multivariate polynomial $\phi_k(\xi) = \phi_{k_1}^1(\xi_1) \cdots \phi_{k_s}^s(\xi_s)$, for $k_1, \ldots, k_s \geq 0$ and $k_1 + \ldots + k_s \leq p$. The integer k, $1 \leq k \leq P = (p+s)!/(p!s!)$, is associated bijectively to the multi-index $(k_1, \ldots, k_s)$, with $k = 1$ associated to $(0, \ldots, 0)$ and $\phi_1 = 1$. Note that $\{\phi_k(\xi)\}_{k=1}^P$ are orthogonal in $\mathrm{L}^2_{f_\xi}$, where $f_\xi = \prod_{i=1}^s f_{\xi_s}$, by independence.

If $\xi_1, \ldots, \xi_s$ are not independent, we define $\phi_k^i(\xi_i) = \xi_i^k$, $k \geq 0$. We define the s-multivariate polynomial $\phi_k(\xi) = \phi_{k_1}^1(\xi_1) \cdots \phi_{k_s}^s(\xi_s)$, for $k_1, \ldots, k_s \geq 0$ and $k_1 + \ldots + k_s \leq p$. The integer k, $1 \leq k \leq P = (p+s)!/(p!s!)$, corresponds bijectively to the multi-index $(k_1, \ldots, k_s)$, with $k = 1$ associated to $(0, \ldots, 0)$. The sequence $\{\phi_k(\xi)\}_{k=1}^P$ is the canonical basis of s-multivariate polynomials in ξ of degree less than or equal to p [20]. Here no orthogonality relations hold.

The stochastic process $x(t)$ has a mean square expansion $x(t) = \sum_{k=1}^\infty \hat{x}_k(t)\phi_k(\xi)$ when p (and so P) tends to infinity, where $\hat{x}_k(t) = (\hat{x}_{k,1}(t), \ldots, \hat{x}_{k,q}(t)) \in \mathbb{R}^q$ are the deterministic coefficients of the expansion. When $\xi_1, \ldots, \xi_s$ are independent, this is referred to as the gPC expansion of $x(t)$, where the Fourier coefficients $\hat{x}_k(t)$ are given by $\hat{x}_k(t) = \mathbb{E}[x(t)\phi_k(\xi)]/\mathbb{E}[\phi_k(\xi)^2]$.

The expansion coefficients $\hat{x}_k(t)$ are unknown. One approximates the solution using Galerkin projections as $x(t) \approx x^P(t) = \sum_{k=1}^P \hat{x}_k^P(t)\phi_k(\xi)$ instead, where $\hat{x}_k^P(t) = (\hat{x}_{k,1}^P(t), \ldots, \hat{x}_{k,q}^P(t)) \in \mathbb{R}^q$ are deterministic coefficients to be found from (1), different from $\hat{x}_k(t)$. The stochastic Galerkin procedure seeks the solution $\{\hat{x}_k^P(t)\}_{k=1}^P$ to

$$\begin{cases} \sum_{k=1}^P \frac{\mathrm{d}}{\mathrm{d}t}\hat{x}_k^P(t)\mathbb{E}[\phi_k(\xi)\phi_l(\xi)] = \mathbb{E}[F(t, \sum_{k=1}^P \hat{x}_k^P(t)\phi_k(\xi), \eta)\phi_l(\xi)], \ t \in I, \\ \sum_{k=1}^P \hat{x}_k^P(t_0)\mathbb{E}[\phi_k(\xi)\phi_l(\xi)] = \mathbb{E}[x_0\phi_l(\xi)], \ 1 \leq l \leq P. \end{cases} \tag{2}$$

This is a system of P coupled deterministic differential equations, which is solvable on I via numerical methods. Let $G = (\mathbb{E}[\phi_k(\xi)\phi_l(\xi)])_{1 \leq k,l \leq P}$ be the Gram matrix of the inner product. When $\xi_1, \ldots, \xi_s$ are independent, then G is the $P \times P$ identity matrix and no ill-conditioning problems of G appear.

In general, $\mathbb{E}[|x(t) - x^P(t)|^2] \to 0$ as $p, P \to \infty$, for each $t \in I$, at spectral rate. Spectral convergence rate means that the decay of the error with p depends on the smoothness of $x(t)$ with respect to the input parameters $\xi_1, \ldots, \xi_s$. If $x(t)$ is of class C^∞ with respect to $\xi_1, \ldots, \xi_s$, then the Galerkin projection $x^P(t)$ converges to $x(t)$ at exponential rate with p. See [12, pp. 33–35] for a detailed discussion.

The componentwise expectation and variance of $x(t)$, $\mathbb{E}[x(t)]$ and $\mathbb{V}[x(t)]$, are approximated from $\mathbb{E}[x^P(t)]$ and $\mathbb{V}[x^P(t)]$, using the formulas

$$\mathbb{E}[x^P(t)] = \sum_{k=1}^P \hat{x}_k^P(t)\mathbb{E}[\phi_k(\xi)], \ \mathbb{V}[x^P(t)] = \sum_{k,l=1}^P \hat{x}_k^P(t)\hat{x}_l^P(t)\left(G_{k,l} - \mathbb{E}[\phi_k(\xi)]\mathbb{E}[\phi_l(\xi)]\right) \tag{3}$$

(here the product of vectors in $\mathbb{R}^q$ is understood componentwise). When $\{\phi_k(\xi)\}_{k=1}^P$ are orthogonal, simpler formulas exist: $\mathbb{E}[x^P(t)] = \hat{x}_1^P(t)$ and $\mathbb{V}[x^P(t)] = \sum_{k=2}^P (\hat{x}_k^P(t))^2\mathbb{E}[\phi_k(\xi)^2]$.

We approximate $f_i(x,t)$, $x \in \mathbb{R}$, using the density function of $x_i^P(t)$, $f_i^P(x,t)$, given a fixed $1 \leq i \leq q$. We propose a computational method based on the RVT technique. Fixed $t \in I$, the random variable $x_i^P(t)$ is a transformation of ξ, $\tilde{g}_t^i(\xi) = \sum_{k=1}^P \hat{x}_{k,i}^P(t)\phi_k(\xi)$. We denote $\xi' = (\xi_1, \ldots, \xi_{s-1})$. Let $g_t^i(\xi) = (\xi', \tilde{g}_t^i(\xi))$. Marginalizing, we have

$$f_i^P(x,t) = \int_{\mathbb{R}^{s-1}} f_{g_t^i(\xi)}(\xi', x)\,\mathrm{d}\xi'. \tag{4}$$

Multidimensional integrals can be approximated using a set of structured nodes, by means of tensor and sparse tensor constructions. Also using cubature rules based on different node locations and weights [12, 42, 43, 44]. Let $\Theta \subseteq \mathbb{R}^{s-1}$ be the set of nodes of interest to approximate (4). Just to put an example: if the supports of $\xi_1, \ldots, \xi_{s-1}$ are bounded and the uncertainty dimension s is low, a cubature rule constructed using a tensor product approach based on univariate Gauss-Legendre quadrature rules can be applied. Univariate Gauss quadratures of Q nodes are exact for polynomials of degree $2Q-1$; they yield the highest possible polynomial degree of exactness (i.e. no other quadrature based on Q nodes integrates polynomials of degrees up to $2Q-1$ exactly).

Other formulations for the transformation mapping $g_t^i(\xi)$ could be used. One should select the formulation that yields the easiest multidimensional integral when computing the marginal (4).

Fix $x \in \mathbb{R}$. For each $\xi' \in \Theta$, we compute the real roots of the univariate polynomial equation $\tilde{g}_t^i(\xi', y) = x$ in y. Let $R_{\xi',x}$ be the set of such roots (it might be empty). Then the following RVT identity holds (see the forthcoming Remarks 2.1 and 2.2):

$$f_{g_t^i(\xi)}(\xi', x) = \sum_{y \in R_{\xi',x}} \frac{f_\xi(\xi', y)}{|\partial_s \tilde{g}_t^i(\xi', y)|} \tag{5}$$

(note that $Jg_t^i(\xi', y) = \partial_s \tilde{g}_t^i(\xi', y)$). As a consequence, from (4), $f_i^P(x,t)$ can be approximated using an integration rule based on $\{f_{g_t^i(\xi)}(\xi', x) : \xi' \in \Theta\}$. The approximations for different $x \in \mathbb{R}$ yield an approximation for the function $f_i^P(\cdot, t)$.

This methodology is summarized in Algorithm 1. Its set of inputs consists of the random differential equation problem (1) under study, the degree p of the polynomial bases, the variable $t \in I$, the discretized domain $\mathcal{S}$ of $f_i(\cdot, t)$, and the integration rule I-R with its set of nodes Θ to approximate the marginal (4). The algorithm returns the list of approximations $\{f_i^P(x,t) : x \in \mathcal{S}\}$.

Algorithm 1 Approximation of the density $f_i(x,t)$ of $x_i(t)$.

procedure DENSITY(RDE, p, t, $\mathcal{S}$, Θ, I-R)
inputs: RDE (random differential equation) problem (1) with s random parameters, degree p, variable $t \in I$, discretization vector $\mathcal{S}$ of the density domain $f_i(x,t)$, set of nodes Θ for the integration rule I-R on the support of ξ'.
    Find the expansion $\tilde{g}_t^i(\xi) = \sum_{k=1}^P \hat{x}_{k,i}^P(t)\phi_k(\xi) = x_i^P(t)$ for $x_i(t)$ ▷ see (2)
    for $x \in \mathcal{S}$ **do**
        for $\xi' \in \Theta$ **do**
            Set $R_{\xi',x} = \{y \in \mathbb{R} : \tilde{g}_t^i(\xi', y) = x\}$
            Set $f_{g_t^i(\xi)}(\xi', x) = \sum_{y \in R_{\xi',x}} \frac{f_\xi(\xi', y)}{|\partial_s \tilde{g}_t^i(\xi', y)|}$ ▷ see (5)
        end for
        Set $f_i^P(x,t)$ according to I-R based on $\{f_{g_t^i(\xi)}(\xi', x) : \xi' \in \Theta\}$ ▷ see (4)
    end for
    return $\{f_i^P(x,t) : x \in \mathcal{S}\}$
end procedure

In practice, the output of Algorithm 1 should be validated. Firstly, one should check that $\int_{\mathbb{R}} f_i^P(x,t)\,\mathrm{d}x = 1$. And secondly, one should compare the expectation and the variance from $f_i^P(x,t)$ with (3) and Monte Carlo simulation on (1). If these consistency conditions do not hold, it indicates a likely implementation error or an insufficient set of integration nodes Θ. The

integrals on dx for $f_i^P(x,t)$ may be computed numerically based on the discretization $\mathcal{S}$ or any other set of nodes.

The complexity of Algorithm 1 is related to the cost of deriving the polynomial expansion of $x_i(t)$ (computing expectations of random polynomials, which depends on the distributions, and solving (2)), the cardinality of $\mathcal{S}$, the cost of the integration rule I-R and the number of its nodes Θ, and the cost of solving polynomial equations of degree p. Thus, if p, s or the number of nodes in $\mathcal{S}$ or Θ grow, the complexity of Algorithm 1 becomes seriously affected.

In fact, the total cost of Algorithm 1 can be explicitly written. Let $\mathcal{G}(\mathrm{RDE}(s),p)$ be the cost of deriving and solving (2) for a random differential equation problem RDE (1) with s random parameters and polynomial bases truncated to degree p. Let $\mathcal{P}_p$ be the cost of solving a polynomial equation of degree p in the real field (cost of finding $R_{\xi',x}$). Let $\mathcal{E}$ be the cost of each fraction in the sum (5), so that (5) requires $p\mathcal{E}$ operations, where p bounds the cardinality of every $R_{\xi',x}$. Denote by $|\mathcal{S}|$ and $|\Theta|$ the cardinality of these sets. Then the cost of Algorithm 1 is

$$O\left(\mathcal{G}(\mathrm{RDE}(s),p)+|\mathcal{S}||\Theta|\left(\mathcal{P}_p+2p\mathcal{E}\right)\right). \tag{6}$$

Remark 2.1. Expression (5) is defined for almost every $(\xi',x)\in\mathbb{R}^{s-1}\times\mathbb{R}$. Indeed, let us see that the problematic set $U=\{(\xi',x):\ x=\tilde{g}_t^i(\xi',y),\ \partial_s\tilde{g}_t^i(\xi',y)=0 \text{ for some } y\in\mathbb{R}\}$ has Lebesgue measure 0 in $\mathbb{R}^s$. We rewrite U as $U=\cup_{\xi'\in\mathbb{R}^{s-1}}\{(\xi',x):\ x\in\Delta_{\xi'}\}$, where $\Delta_{\xi'}=\{x\in\mathbb{R}:\ x=\tilde{g}_t^i(\xi',y),\ y\in\mathcal{V}_{\xi'}\}$ and $\mathcal{V}_{\xi'}$ is the set of real roots of $\partial_s\tilde{g}_t^i(\xi',y)=0$. Since the cardinality of $\mathcal{V}_{\xi'}$ is $\leq p-1$, $\Delta_{\xi'}$ has Lebesgue measure 0 in $\mathbb{R}$. Then, by Fubini's theorem, U has Lebesgue measure 0 in $\mathbb{R}^s$, as wanted.

Remark 2.2. The identity (5) can be easily justified using properties of the Dirac delta function $\delta(x)$. First, from the definition of conditional density function, we have:

$$f_{g_t^i(\xi',\xi_s)}(\eta',\eta_s)=f_{(\xi',\tilde{g}_t^i(\xi',\xi_s))}(\eta',\eta_s)=f_{\tilde{g}_t^i(\xi',\xi_s)|\xi'=\eta'}(\eta_s)f_{\xi'}(\eta')=f_{\tilde{g}_t^i(\eta',\xi_s)|\xi'=\eta'}(\eta_s)f_{\xi'}(\eta'),$$

for $(\eta',\eta_s)\in\mathbb{R}^{s-1}\times\mathbb{R}$. Now we compute $f_{\tilde{g}_t^i(\eta',\xi_s)}(\eta_s)$. By using the identity $f_V(v)=\mathbb{E}[\delta(V-v)]$ for any random variable V [45], we write

$$f_{\tilde{g}_t^i(\eta',\xi_s)|\xi'=\eta'}(\eta_s)=\mathbb{E}\left[\delta\left(\tilde{g}_t^i(\eta',\xi_s)-\eta_s\right)|\xi'=\eta'\right].$$

By [46, Remark 2.3],

$$\delta\left(\tilde{g}_t^i(\eta',\xi_s)-\eta_s\right)=\sum_{z\in R_{\eta',\eta_s}}\frac{\delta(\xi_s-z)}{|\partial_s\tilde{g}_t^i(\eta',z)|},$$

where $R_{\eta',\eta_s}=\{z\in\mathbb{R}:\ \tilde{g}_t^i(\eta',z)=\eta_s\}$. Hence, by the linearity of the expectation,

$$f_{\tilde{g}_t^i(\eta',\xi_s)|\xi'=\eta'}(\eta_s)=\sum_{z\in R_{\eta',\eta_s}}\frac{\mathbb{E}[\delta(\xi_s-z)|\xi'=\eta']}{|\partial_s\tilde{g}_t^i(\eta',z)|}=\sum_{z\in R_{\eta',\eta_s}}\frac{f_{\xi_s|\xi'=\eta'}(z)}{|\partial_s\tilde{g}_t^i(\eta',z)|}.$$

We thus deduce the required formula:

$$f_{g_t^i(\xi',\xi_s)}(\eta',\eta_s)=\sum_{z\in R_{\eta',\eta_s}}\frac{f_{\xi_s|\xi'=\eta'}(z)f_{\xi'}(\eta')}{|\partial_s\tilde{g}_t^i(\eta',z)|}=\sum_{z\in R_{\eta',\eta_s}}\frac{f_{\xi}(\eta',z)}{|\partial_s\tilde{g}_t^i(\eta',z)|}.$$

Remark 2.3. In the particular case of one random input parameter in (1) ($s = 1$), which was the case studied in [34], Algorithm 1 is applicable with no ξ' and no integration rule I-R. There is only one "for" loop over $\mathcal{S}$, and ξ' is substituted by a blank space. The total cost (6) of the algorithm becomes $O(\mathcal{G}(\mathrm{RDE}(1), p) + |\mathcal{S}|(\mathcal{P}_p + p\mathcal{E}))$.

In the following examples, we demonstrate the accuracy of the method proposed. In many situations, our approach shows a significant advantage compared to other stochastic methods. Nonetheless, its strength is problem-dependent.

Example 2.4. This example illustrates the convergence of Algorithm 1 for a simple model:

$$\begin{cases} x'(t) = \alpha x(t), \ t \in \mathbb{R}, \\ x(0) = \beta, \end{cases} \tag{7}$$

where β and α are regarded as random variables. We assume that they follow a Normal$(0, 1)$ distribution and that they are independent. As the exact solution is known, $x(t) = \beta \mathrm{e}^{\alpha t}$, its probability density function can be computed using the RVT method, which yields $f(x, t) = \int_{\mathbb{R}} f_\alpha(\alpha) f_\beta(x\mathrm{e}^{-\alpha t})\mathrm{e}^{-\alpha t}\,\mathrm{d}\alpha$, $x \in \mathbb{R}$. We test Algorithm 1. We denote $\xi = (\xi', \xi_2) = (\beta, \alpha)$ ($s = 2$). For different p and $P = (p + s)!/(p!s!)$, we compute the Galerkin projections $x^P(t)$ as linear combinations of tensor Hermite polynomials in ξ (these polynomials form the PC basis functions). As integration rule I-R, we take the one-dimensional Gauss-Hermite quadrature rule of degree Q with weight function f_β. The set of nodes Θ is formed by the zeros of the Q-th degree Hermite polynomial. In Figure 1, we plot $e^p(t = 0.5) = \|f(\cdot, t = 0.5) - f^P(\cdot, t = 0.5)\|_\infty$ for $Q = 25$, where $f^P(x, t)$ is the density function of $x^P(t)$ computed with Algorithm 1. This kind of semi-log plot allows observing graphically the exponential convergence of the densities with p. Figure 1 also depicts the max-norm of the error arising from a non-parametric smooth kernel density estimation using M simulations (with Silverman's rule to determine the bandwidth, given by $0.9\hat{\sigma}_{x(t)}M^{-1/5}$, where $\hat{\sigma}_{x(t)}$ is the Monte Carlo estimate of the standard deviation of $x(t)$, and with Gaussian kernel), $\epsilon^M(t = 0.5)$, in log-log scale (the solid line is the estimated mean max-norm and the dashed lines refer to the estimated 5% and 95% quantiles of the max-norm). We see that the kernel estimation cannot achieve the convergence regime of the spectral methods. The error $\epsilon^M(t = 0.5)$ decreases with M as $\propto M^{-\rho}$, $\rho \approx 0.37$. The Monte Carlo simulation is a collocation method, i.e. from local information on the solution (realizations) one must determine its global variability, so the method is limited in terms of efficiency [23, Section 1.4.2]. Kernel density estimations are non-parametric methods whose rate of convergence with the number of simulations M is slow, of the order $M^{-\gamma}$, for certain $0 < \gamma < 1/2$ (the popular convergence rate $M^{-1/2}$ corresponds to a parametric Monte Carlo estimation of the mean parameter) [47, 48, 49]. For instance, according to [47], if the target density function is Γ-Hölder continuous, $\Gamma \in (0, 1]$, then the pointwise convergence rate is $\leq O(M^{-\gamma})$, where $\gamma = \Gamma/(2\Gamma + 1)$. When the target density is sufficiently smooth so that $\Gamma = 1$, then $\gamma = 1/3 \approx \rho$, which agrees with the numerical experiment conducted here. Moreover, if the unknown density function is heavy-tailed (e.g. the log-normal distribution), possesses peaks or discontinuity points (e.g. the uniform distribution), etc. then the kernel density approach may induce significant error estimates. By contrast, the spectral methods reconstruct the functional dependence of the solution on the input coefficients, usually in terms of a series, which permits determining its statistics and its density function analytically and correctly capturing density features.

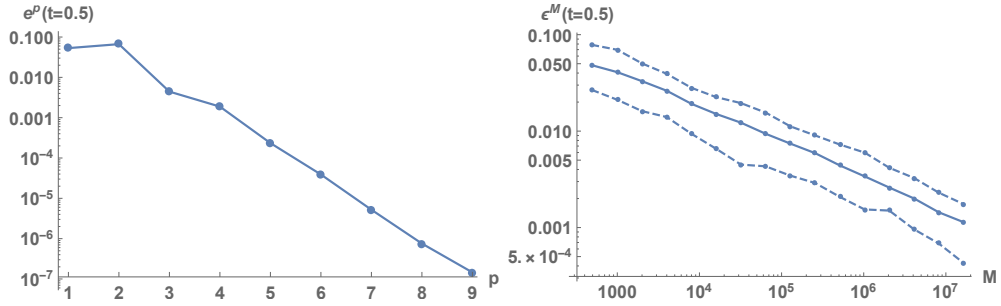

Figure 1: First panel: Error $e^p(t = 0.5) = \|f(\cdot, t = 0.5) - f^P(\cdot, t = 0.5)\|_\infty$ of the algorithm for quadrature degree $Q = 25$ and different p. Second panel: Max-norm of the error arising from a smooth kernel density estimation using M simulations, $\epsilon^M(t = 0.5)$ (the solid line is the estimated mean max-norm and the dashed lines refer to the estimated 5% and 95% quantiles of the max-norm). This figure corresponds to Example 2.4.

Example 2.5. We consider (7), where $\xi = (\xi', \xi_2) = (\beta, \alpha) \sim$ Dirichlet$(1.5, 1.5, 1.5)$. The exact density function of $x(t)$, $f(x, t) = \int_{\mathbb{R}} f_{(\alpha,\beta)}(\alpha, x\mathrm{e}^{-\alpha t})\mathrm{e}^{-\alpha t}\,\mathrm{d}\alpha$, is plotted for $t = 0.5$ in the first panel of Figure 2, together with a kernel density estimation using $20,000,000$ simulations. We observe that $f(x, t = 0.5)$ has the non-differentiability point $x = 0$; then the kernel density estimate smooths out the approximation and draws a tail. Our approach based on polynomial expansions and the RVT method does not present such problem. In Algorithm 1, we consider polynomial approximations of $x(t)$: $x^P(t)$ for $P = (p + s)!/(p!s!)$, $s = 2$ and distinct basis orders p, where $x^P(t)$ is a linear combination of the canonical basis $\alpha^i\beta^j$, $i, j \geq 0$, $i + j \leq p$. As I-R, we take the Gauss-Legendre quadrature rule on $[0, 1]$ of degree Q, and Θ is the set of zeros of the Q-th degree Legendre polynomial. Figure 2, second panel, depicts the error $e^p(t = 0.5) = \|f(\cdot, t = 0.5) - f^P(\cdot, t = 0.5)\|_\infty$ in semi-log scale. These errors decrease to zero exponentially with p, until the error due to the quadrature rule I-R is reached. The rate of convergence of the quadrature rule I-R with Q depends on the smoothness of the corresponding integrand: from exponential convergence if it is analytic, to maybe sub-algebraic convergence (i.e. error decay slower than Q^{-1}) if it is merely continuous; and if the integrand is smooth with large derivatives (sharp peaks, which may occur if the variances of the inputs are small), then the convergence rapidity deteriorates. For instance, the convergence of the quadrature rule I-R with Q in Example 2.4 was much faster than in this example.

Example 2.6. We consider (7) with independent inputs $\beta, \alpha \sim$ Uniform$(0, 1)$. The exact density function of the solution $x(t)$, $f(x, t) = \int_{\mathbb{R}} f_\alpha(\alpha) f_\beta(x\mathrm{e}^{-\alpha t})\mathrm{e}^{-\alpha t}\,\mathrm{d}\alpha$, is plotted at $t = 0.5$ in Figure 3, first panel. Observe the discontinuity point at $x = 0$ and the other two non-differentiability points. We demonstrate in this example that Algorithm 1 is able to identify these discontinuities and peaks, in contrast to kernel-based methods. The procedure here is analogous to Example 2.4, but the gPC basis functions consist of tensor Legendre polynomials on $[0, 1] \times [0, 1]$ and I-R is the Gauss-Legendre quadrature rule on $[0, 1]$ of degree Q. Figure 3, second panel, depicts the error $e^p(t = 0.5) = \|f(\cdot, t = 0.5) - f^P(\cdot, t = 0.5)\|_\infty$ in semi-log scale. As occurred in Example 2.5, the decay of the error to zero is exponential with p, until the error due to the quadrature rule I-R dominates. For $p = 3$, the error due to the Galerkin approximation is already smaller than the quadrature error for $Q = 180$, so for $p \geq 3$ the density approximations do not improve. The numerical quadrature I-R converges slowly with Q because of the discontinuity

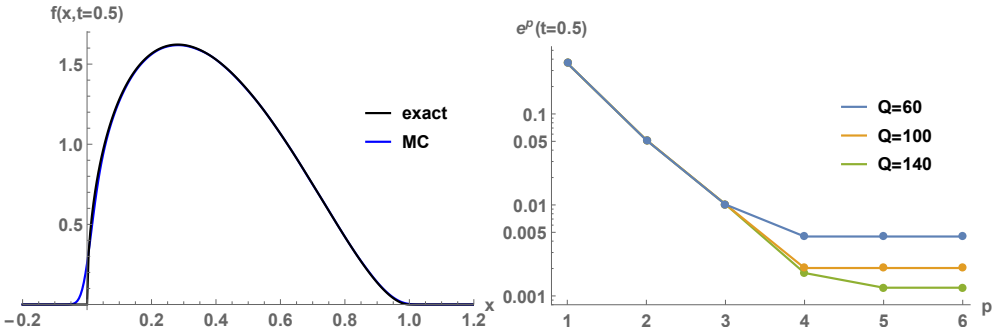

Figure 2: First panel: Exact density function $f(x, t = 0.5)$ and a kernel density estimation using $20,000,000$ Monte Carlo simulations (MC). Second panel: Error $e^p(t = 0.5) = \|f(\cdot, t = 0.5) - f^p(\cdot, t = 0.5)\|_\infty$ of the algorithm for different quadrature degrees Q and different basis orders p. This figure corresponds to Example 2.5.

of the corresponding integrand. In these cases, the integration scheme I-R may slow down the convergence of the algorithm severely and we may not benefit from the spectral convergence of the Galerkin projections. Nonetheless, good pointwise approximations to the target density with error of the order of 10^{-3} are still possible. The third panel of Figure 3 plots the error $e^p(t = 0.5)$ of the algorithm for $Q = 600$ and different p. The error reaches 10^{-3}. For $p \geq 4$ the quadrature error dominates and $e^p(t = 0.5)$ becomes constant with p.

Example 2.7. This example is devoted to the study of two pathological cases. The gPC and Galerkin-based methods have been extensively used in the recent years to approximate the statistical moments of random variables. However, from a theoretical standpoint, the series representations of the random variable only converge in the mean square sense. As shown in [50], it is possible to find examples of random quantities whose gPC approximations do not converge in certain Lebesgue space L^r, $r > 2$. For instance, if $X = \Phi(Z)$, where $Z \sim \text{Normal}(0, 1)$, Φ is the cumulative distribution function of Z and $X \sim \text{Uniform}(0, 1)$, then the PC expansion of X in terms of the Hermite polynomials evaluated at Z does not converge in the mean fourth sense. The same occurs for $X = |Z|$, where $Z \sim \text{Normal}(0, 1)$. In these two cases, the PC expansions of X are available via closed-form expressions, see [50]. We aim at analyzing the convergence of Algorithm 1 for these two situations. As there is only one random parameter $\xi = Z$, the simplifications for the algorithm explained in Remark 2.3 apply. Figure 4 shows the errors $e^p = \|f - f^p\|_\infty$ of the algorithm in semi-log scale for $X = \Phi(Z)$ (first panel) and $X = |Z|$ (second panel), where f is the exact density function of X and f^p is the density function of the PC expansion of X truncated at order p. In the first plot, we clearly observe exponential convergence with p. By contrast, the second plot does not show convergence, at least for $p \leq 50$; either there is no convergence or the convergence is very slow as $p \to \infty$. The main difficulty in the gPC approximation of the absolute value comes from its lack of differentiability at zero [23, Section 4.5.4].

3. Application to the SIR epidemic model

In the SIR (susceptible-infected-recovered) epidemiological model, the population is divided into compartments according to the disease stage: $S(t)$, $I(t)$ and $R(t)$ denote the proportion of

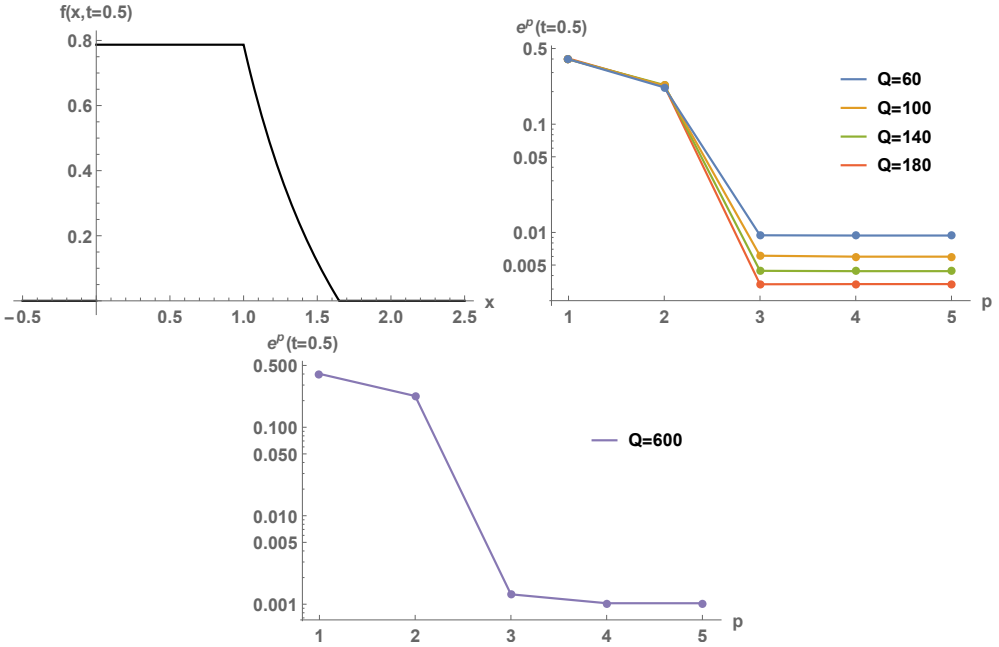

Figure 3: First panel: Exact density function $f(x, t = 0.5)$. Second panel: Error $e^p(t = 0.5) = \|f(\cdot, t = 0.5) - f^P(\cdot, t = 0.5)\|_\infty$ of the algorithm for different quadrature degrees Q and different basis orders p. Third panel: Error $e^p(t = 0.5)$ of the algorithm for quadrature degree $Q = 600$ and different p. This figure corresponds to Example 2.6.

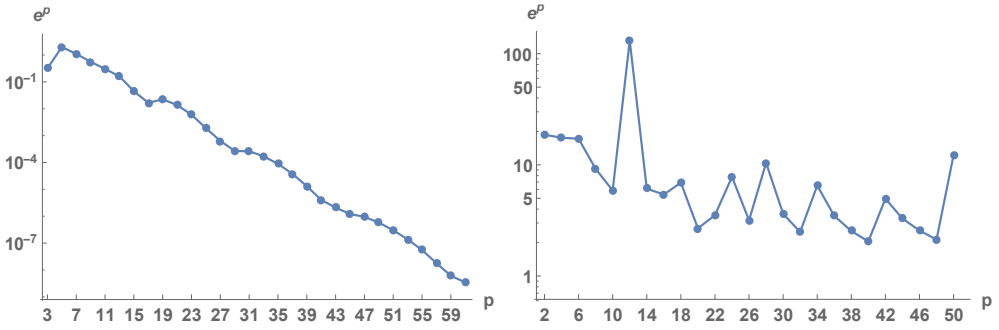

Figure 4: Errors $e^p = \|f - f^p\|_\infty$ of the algorithm for the random variables $X = \Phi(Z)$ (first panel) and $X = |Z|$ (second panel), for different basis orders p. This figure corresponds to Example 2.7.

susceptible, infected and recovered individuals at time t, respectively. There are several assumptions that characterize the SIR model. There is homogeneous mixing, that is, all individuals are equally likely to contact any other individual. The population is constant, by assuming no vital dynamics (no births, no deaths). Finally, it is assumed that there is lasting immunity after infection. The mathematical model is the following system of quadratic differential equations:

$$\begin{cases} S'(t) &= -\gamma S(t)I(t), \\ I'(t) &= \gamma S(t)I(t) - \delta I(t), \\ R'(t) &= \delta I(t), \end{cases} \tag{8}$$

where $\gamma > 0$ and $\delta > 0$ are the contact and the recovery rates, respectively. The initial conditions are $S(0) = S_0$, $I(0) = 1 - S_0$ and $R(0) = 0$.

Let us assume that $\delta > 0$, $\gamma > 0$ and $S_0 \in [0, 1]$ are random variables. Let $\xi = (\xi_1, \xi_2, \xi_3) = (\delta, \gamma, S_0)$. We aim at approximating the probability density functions $f_S(x,t)$, $f_I(x,t)$ and $f_R(x,t)$, at time $t \geq 0$. No solution has been presented in the literature, due to (8) not having a simple closed-form solution to apply the RVT method. Only very recently, the RVT technique has been applied to an approximate solution (by linearization) to (8) [41], although the approximations to $f_S(x,t)$, $f_I(x,t)$ and $f_R(x,t)$ obtained in such a way may not be accurate.

In the following examples, we approximate successfully $f_S(x,t)$, $f_I(x,t)$ and $f_R(x,t)$ using Algorithm 1. We set different probability distributions to (δ, γ, S_0), based on independent and non-independent distributions, to test our methodology. Such probability distributions should match the epidemiological interpretation (boundedness, positiveness, etc.).

Example 3.1. Set the distributions $\delta \sim \text{Normal}(0.6, \sigma^2 = 0.005)|_{[0,1]}$, $\gamma \sim \text{Exponential}(20)|_{[0,1]}$ and $S_0 \sim \text{Beta}(1200, 400)$. The distributions of δ and γ are truncated to $[0, 1]$. These three random inputs are assumed to be independent. These distributions were tested in [41].

We apply the stochastic Galerkin technique with gPC basis functions based on orthogonal polynomials constructed via Gram-Schmidt orthogonalization procedures, for degrees $p \in \{1, 2, 3\}$. We obtain polynomial representations for $S(t)$, $I(t)$ and $R(t)$; let us denote them by $S^P(t)$, $I^P(t)$ and $R^P(t)$, where $P = (p+s)!/(p!s!)$, $s = 3$.

We focus on $f_S(x,t)$. Let $\tilde{g}_t^i(\xi) = S^P(t)$, $\xi = (\delta, \gamma, S_0)$, and $\xi' = (\delta, \gamma)$. The marginal density (4) is an integral on $[0,1] \times [0,1]$ with respect to δ and γ. As I-R, we use a cubature rule constructed using a tensor product approach based on univariate Gauss-Legendre quadrature rules, each one of degree Q. The set of nodes Θ is given by $\Theta_1 \times \Theta_2$, where $\Theta_1 = \Theta_2$ consist of the roots of the Q-th degree Legendre polynomial on $[0, 1]$.

In Figure 5, we plot $f_S(x, t = 1)$ for degrees $p = 1, 2, 3$, with quadrature degree $Q = 20$. Observe that convergence is achieved for small p, due to the fast convergence of the Galerkin projections. The right panel is a zoom where we compare our approximations for $p = 1, 2, 3$ with the approximation from [41]. Notice that the method from [41] gives rise to errors in the estimates. Figure 6 is analogous for time $t = 2$.

In Figure 7, we analyze the accuracy of the quadrature rule with Q, for $p = 3$. We observe that $Q = 20$ gives essentially error-free double integrals. For $Q \leq 10$, a significant error is perceptible. In general, one should analyze carefully which Q gives accurate approximations, as this accuracy is problem-dependent.

To complete the computations of the densities, Figure 8 depicts $f_I(x, t = 1)$ and $f_R(x, t = 1)$ for $p = 1, 2, 3$, and for $Q = 25$ and $Q = 30$ respectively. One selects Q such that the convergence of the quadrature rule has been achieved; this depends on the response process under study.

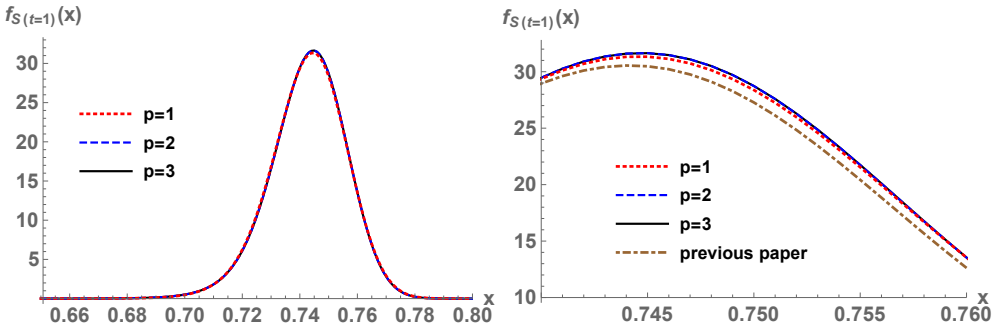

Figure 5: Approximation of $f_S(x, t = 1)$ for degrees $p = 1, 2, 3$, with quadrature degree $Q = 20$. The right panel is a zoom where the approximation from [41] is also represented. This figure corresponds to Example 3.1.

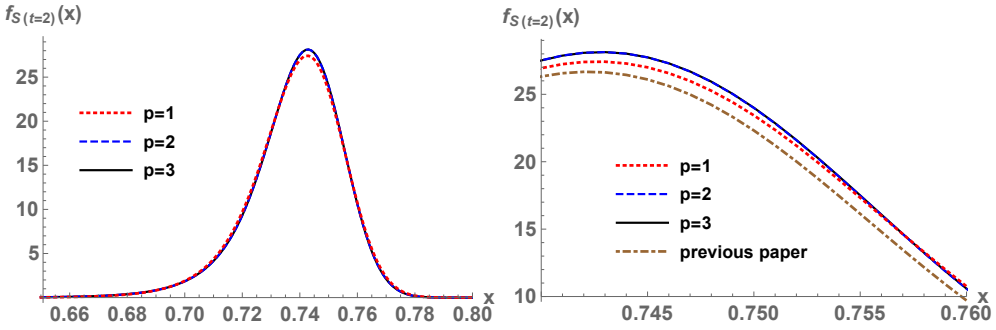

Figure 6: Approximation of $f_S(x, t = 2)$ for degrees $p = 1, 2, 3$, with quadrature degree $Q = 20$. The right panel is a zoom where the approximation from [41] is also represented. This figure corresponds to Example 3.1.

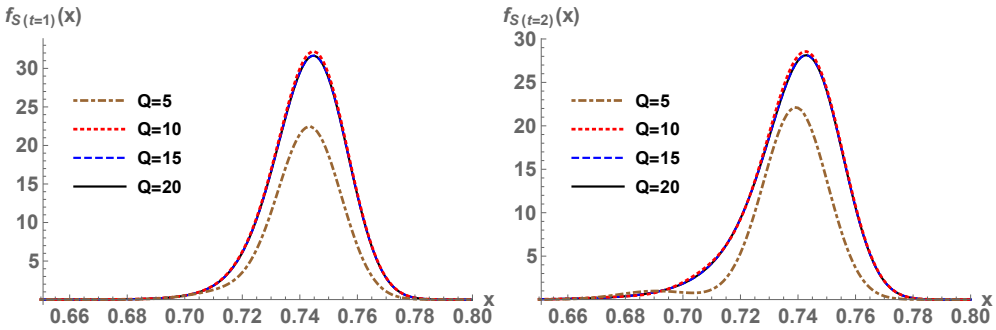

Figure 7: Approximation of $f_S(x, t = 1)$ (first) and $f_S(x, t = 2)$ (second) for different quadrature degrees Q and $p = 3$. This figure corresponds to Example 3.1.

In the case of $f_R(x, t = 1)$, we also plot the density derived from [41] in order to show our improvements. In Figure 9 we analyze graphically the convergence of the quadrature rule with Q, for $p = 3$ fixed.

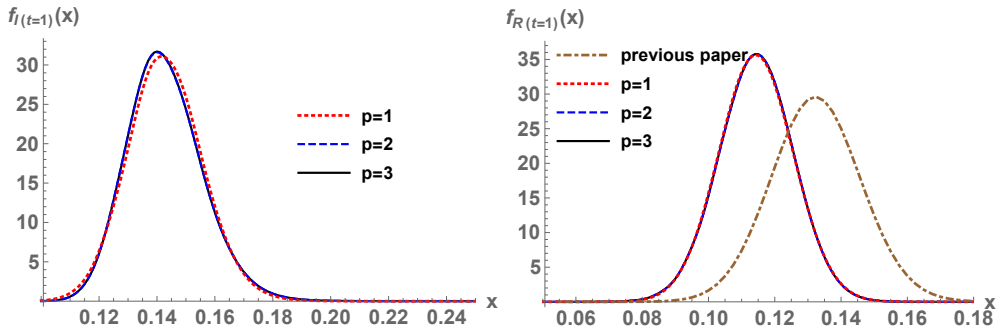

Figure 8: Approximation of $f_I(x, t = 1)$ (first) and $f_R(x, t = 1)$ (second) for $p = 1, 2, 3$, $Q = 25$ (for I) and $Q = 30$ (for R). The approximation using the method from [41] is also plotted. This figure corresponds to Example 3.1.

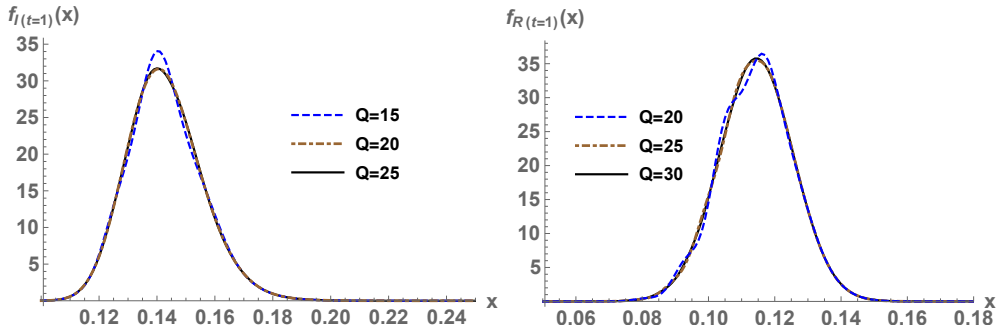

Figure 9: Approximation of $f_I(x, t = 1)$ (first) and $f_R(x, t = 1)$ (second) for different quadrature degrees Q and $p = 3$. This figure corresponds to Example 3.1.

Example 3.2. Let us consider $(\delta, \gamma) \sim$ Dirichlet$(80, 4, 316)$ and $S_0 \sim$ Beta$(1200, 400)$, where (δ, γ) and S_0 are assumed to be independent.

Due to the non-independence of the components of ξ, we use canonical polynomial expansions based on $\delta^{k_1}\gamma^{k_2}S_0^{k_3}$, $k_1, k_2, k_3 \geq 0$, $k_1 + k_2 + k_3 \leq p$. For degrees $p \in \{1, 2, 3\}$, we obtain polynomial representations for $S(t)$, $I(t)$ and $R(t)$: $S^P(t)$, $I^P(t)$ and $R^P(t)$, respectively, where $P = (p + s)!/(p!s!)$, $s = 3$. Then the two nested "for" loops from Algorithm 1 are run as in Example 3.1, with $\xi' = (\delta, \gamma)$, I-R being the tensor product of univariate Gauss-Legendre quadratures of degree Q on $[0, 1]$, and $\Theta = \Theta_1 \times \Theta_2$, being $\Theta_1 = \Theta_2$ the set of roots of the Q-th degree Legendre polynomial on $[0, 1]$.

Figure 10 plots the densities $f_S(x, t = 1)$, $f_I(x, t = 1)$ and $f_R(x, t = 1)$, for $p = 1, 2, 3$, $Q = 60$ (for S and I) and $Q = 85$ (for R). This degree Q has been checked to be enough, by densities and statistics comparisons for different quadrature degrees and by validation of the algorithm output,

as in Example 3.1. Intuitively, Q is larger than in Example 3.1 because the variances of the inputs are smaller, therefore the densities involved in the algorithm are more picked. Observe that, once Q is selected, convergence is achieved for small p due to the fast convergence of the polynomial representations. Even for $p = 1$ the estimates obtained are very accurate.

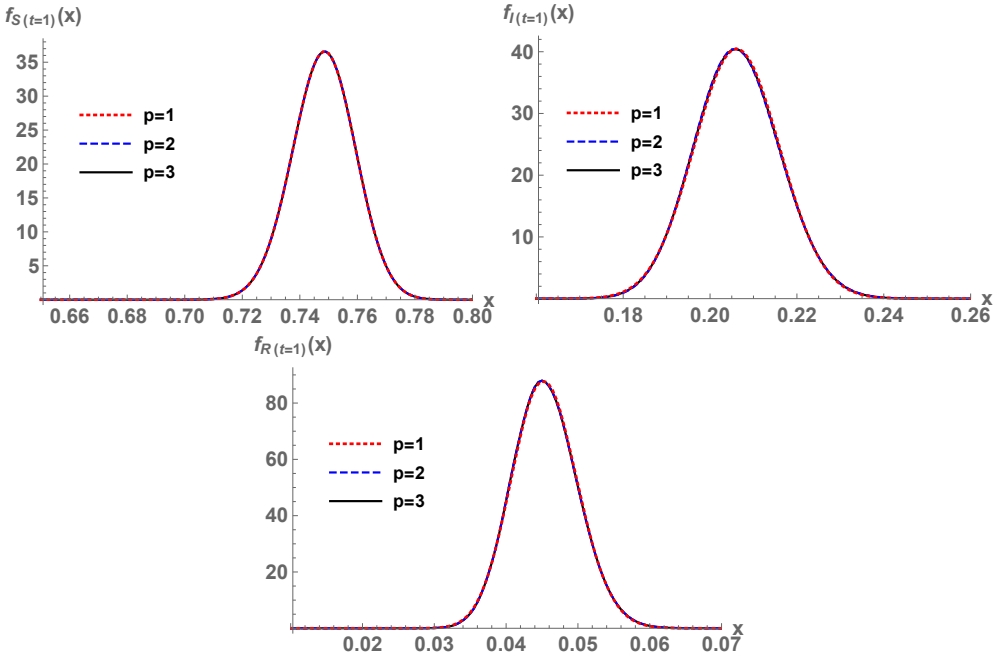

Figure 10: Approximation of $f_S(x, t = 1)$ (first), $f_I(x, t = 1)$ (second) and $f_R(x, t = 1)$ (third) for $p = 1, 2, 3$, $Q = 60$ (for S and I) and $Q = 85$ (for R). This figure corresponds to Example 3.2.

We conclude this example by assessing graphically the convergence of the quadrature rule with Q in Figure 11, for $p = 3$ fixed.

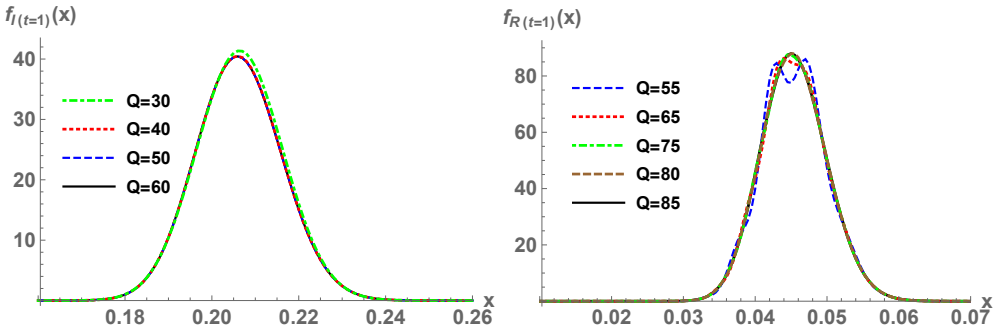

Figure 11: Approximation of $f_I(x, t = 1)$ (first) and $f_R(x, t = 1)$ (second) for different quadrature degrees Q and $p = 3$. This figure corresponds to Example 3.2.

4. Discussion and conclusions

In this paper, we combine polynomial representations and the RVT method to approximate the probability density function of the solution to general complex systems with uncertainties formulated via random differential equations. The differential equations can be non-linear and the random inputs may be non-independent. This paper is very general in dealing with density approximations, as it does not need closed-form solutions and is problem-independent. We take profit of two stochastic methods with very especial features: spectral convergence (for the polynomial expansions) and exact density computation (for the RVT technique). In many situations it improves the classical density estimations that use Monte Carlo simulation and kernel-based methods, in terms of fast density approximations and correctly capturing density features.

Our methodology is applied to the SIR (susceptible-infected-recovered) epidemic model. Given specific probability distributions for the contact and recovery rates and the initial conditions, we approximate the probability density function of the proportion of susceptible, infected and recovered individuals. Our results present significant improvements compared to the existing literature on random differential equations and random epidemic models.

We comment further research that could be conducted in the future. Although polynomial expansions converge rapidly, for certain problems a large polynomial degree p might be required, especially when working at large time t. In such a case, the derivation of the polynomial expansion is more expensive and challenging. Thus, other polynomial representations could be sought.

On the other hand, our algorithm becomes very expensive when the number s of random input parameters is large or the set Θ of integration nodes needs to be increased; it suffers from the so-called curse of dimensionality. First, because of the derivation of the polynomial representation. And second, because of the integration on $\mathbb{R}^{s-1}$ to compute the marginal density function. Efficient numerical integration schemes based on sparse grids should be used in such a case.

Our methodology could be applied to other types of stochastic models arising in Epidemiology, Physics, etc. based on random difference equations, random partial differential equations, random systems with delay, etc. The methods are analogous.

Finally, a theoretical analysis on the validity of the algorithm in general and on the convergence of the density functions as p grows shall be carried out. Essentially, the main question is whether the polynomial expansions presented in the paper converge to the model solution in the total variation distance, i.e. their density functions converge in $\mathrm{L}^1(\mathbb{R})$. A stronger condition is the convergence almost everywhere of the densities.

Acknowledgements

This work has been supported by the Spanish Ministerio de Economía y Competitividad grant MTM2017–89664–P. The author Marc Jornet acknowledges the doctorate scholarship granted by Programa de Ayudas de Investigación y Desarrollo (PAID), Universitat Politècnica de València.

Conflict of Interest Statement

The authors declare that there is no conflict of interests regarding the publication of this article.

[1] Soong TT. Random differential equations in science and engineering. New York: Academic Press; 1973.

[2] Neckel T, Rupp F. Random fifferential equations in scientific computing. München, Germany: Walter de Gruyter; 2013.
[3] Strand JL. Random ordinary differential equations. J Differ Equ 1970;7:538–553.
[4] Smith RC. Uncertainty quantification. Theory, implementation, and application. SIAM Computational Science & Engineering; 2014.
[5] Fishman G. Monte Carlo: Concepts, algorithms, and applications. New York: Springer Science & Business Media; 2013.
[6] Crandall SH. Perturbation techniques for random vibration of nonlinear systems. J Acoust Soc Am 1963;35(11):1700–1705.
[7] Villafuerte L, Chen-Charpentier BM. A random differential transform method: Theory and applications. Appl Math Lett 2012;25(10):1490–1494.
[8] Khan Y, Wu Q. Homotopy perturbation transform method for nonlinear equations using He's polynomials. Comput Math Appl 2011;61(8):1963–1967.
[9] Khan Y, Vázquez-Leal H, Wu Q. An efficient iterated method for mathematical biology model. Neural Comput Appl 2013;23(3-4):677–682.
[10] Ghanem RG, Spanos P. Stochastic finite elements: A spectral approach. New York: Springer-Verlag; 1991.
[11] Xiu D, Karniadakis G. The Wiener-Askey polynomial chaos for stochastic differential equations. SIAM J Sci Comput 2002;24:619–644.
[12] Xiu D. Numerical methods for stochastic computations. A spectral method approach. New York: Cambridge Texts in Applied Mathematics, Princeton University Press; 2010.
[13] Chen-Charpentier BM, Cortés JC, Licea JA, Romero JV, Roselló MD, Santonja FJ, Villanueva RJ. Constructing adaptive generalized polynomial chaos method to measure the uncertainty in continuous models: A computational approach. Math Comput Simulat 2015;109:113–129.
[14] Cortés JC, Romero JV, Roselló MD, Villanueva RJ. Improving adaptive generalized polynomial chaos method to solve nonlinear random differential equations by the random variable transformation technique. Commun Nonlinear Sci Numer Simul 2017;50:1–15.
[15] Ernst OG, Mugler A, Starkloff HJ, Ullmann E. On the convergence of generalized polynomial chaos expansions. ESAIM Math Model Numer Anal 2012;46:317–339.
[16] Shi W, Zhang C. Error analysis of generalized polynomial chaos for nonlinear random ordinary differential equations. Appl Numer Math 2012;62:1954–1964.
[17] Shi W, Zhang C. Generalized polynomial chaos for nonlinear random delay differential equations. Appl Numer Math 2017:115;16–31. 2017.
[18] Calatayud J, Cortés JC, Jornet M. On the convergence of adaptive gPC for non-linear random difference equations: Theoretical analysis and some practical recommendations. J Nonlinear Sci Appl 2018;11(9):1077–1084.
[19] Gottlieb D, Xiu D. Galerkin method for wave equations with uncertain coefficients. Commun Comput Phys 2008;3(2):505–518.
[20] Cortés JC, Romero JV, Roselló MD, Santonja FJ, Villanueva RJ. Solving continuous models with dependent uncertainty: a computational approach. Abstr Appl Anal 2013;2013.
[21] Calatayud J, Cortés JC, Jornet M, Villanueva RJ. Computational uncertainty quantification for random time-discrete epidemiological models using adaptive gPC. Math Method Appl Sci 2018;41:9618–9627.
[22] Calatayud J, Cortés JC, Jornet M. Uncertainty quantification for nonlinear difference equations with dependent random inputs via a stochastic Galerkin projection technique. Commun Nonlinear Sci Numer Simul 2019;72:108–120.
[23] Le Maître OP, Knio OM. Spectral methods for uncertainty quantification: With applications to computational fluid dynamics. Netherlands: Springer Science & Business Media; 2010.
[24] Calatayud J, Cortés JC, Jornet M, Navarro-Quiles A. Solving random ordinary and partial differential equations through the probability density function. Theory and computing with applications. In: Sadovnichiy VA, Zgurovsky M, editors. Modern mathematics and mechanics. Fundamentals, problems and challenges, New York: Springer International Publishing AG; 2019, p. 261–282.
[25] Dorini FA, Cecconello MS, Dorini MB. On the logistic equation subject to uncertainties in the environmental carrying capacity and initial population density. Commun Nonlinear Sci Numer Simul 2016;33:160–173.
[26] Santos LT, Dorini FA, Cunha MCC. The probability density function to the random linear transport equation. Appl Math Comput 2010;216(5):1524–1530.
[27] Hussein A, Selim MM. Solution of the stochastic transport equation of neutral particles with anisotropic scattering using RVT technique. Appl Math Comput 2009;213(1):250–261.
[28] Hussein A, Selim MM. Solution of the stochastic radiative transfer equation with Rayleigh scattering using RVT technique. Appl Math Comput 2012;218(13):7193–7203.
[29] Calatayud J, Cortés JC, Jornet M. The damped pendulum random differential equation: A comprehensive stochastic analysis via the computation of the probability density function. Physica A 2018;512:261–279.

[30] Calatayud J, Cortés JC, Jornet M. Uncertainty quantification for random parabolic equations with non-homogeneous boundary conditions on a bounded domain via the approximation of the probability density function. Math Method Appl Sci 2019;42(17):5649–5667.
[31] Jornet M, Calatayud J, Le Maître OP, Cortés JC. Second order linear differential equations with analytic uncertainties: stochastic analysis via the computation of the probability density function. ArXiv:1909.05907; 2019.
[32] El-Tawil MA. The approximate solutions of some stochastic differential equations using transformations. Appl Math Comput 2005:164(1);167–178.
[33] Calatayud J, Cortés JC, Díaz JA, Jornet M. Density function of random differential equations via finite difference schemes: a theoretical analysis of a random diffusion-reaction Poisson-type problem. Stochastics 2019. https://doi.org/10.1080/17442508.2019.1645849.
[34] Calatayud J, Chen-Charpentier BM, Cortés JC, Jornet M. Combining polynomial chaos expansions and the random variable transformation technique to approximate the density function of stochastic problems, including some epidemiological models. Symmetry 2019;11(1):43.
[35] Hethcote HW. The mathematics of infectious diseases. SIAM Rev 2000;42(4):599–653.
[36] Levin SA, Hallam TG, Gross LJ. Applied mathematical ecology. Berlin, Heidelberg: Springer Science & Business Media; 2012.
[37] Brauer F. Compartmental models in epidemiology. Mathematical epidemiology. Berlin, Heidelberg: Springer; 2008:19–79.
[38] Casabán MC, Cortés JC, Romero JV, Roselló MD. Probabilistic solution of random SI-type epidemiological models using the random variable transformation technique. Commun Nonlinear Sci Numer Simul 2015;24:86–97.
[39] Casabán MC, Cortés JC, Navarro-Quiles A, Romero JV, Roselló MD, Villanueva RJ. A comprehensive probabilistic solution of random SIS-type epidemiological models using the random variable transformation technique. Commun Nonlinear Sci Numer Simul 2016;32:199–210.
[40] Chen-Charpentier BM, Stanescu D. Epidemic models with random coefficients. Math Comput Model 2010;52(7–8):1004–1010.
[41] Slama H, Hussein A, El-Bedwhey NA, Selim MM. An approximate probabilistic solution of a random SIR-type epidemiological model using RVT technique. Appl Math Comput 2019;361:144–156.
[42] Trefethen LN. Is Gauss quadrature better than Cleanshaw-Curtis? SIAM Rev. 2008;50(1):67–87.
[43] Gerstner T, Griebel M. Numerical integration using sparse grids. Numer. Algorithms 1998;18:209–232.
[44] Delves LM, Mohamed JL. Computational methods for integral equations. Cambridge University Press; 1985.
[45] Shvidler M, Karasaki K. Probability density functions for solute transport in random fields. Transp. Porous Media 2003;50:243–266.
[46] Dorini FA, Cunha MCC. On the linear advection equation subject to random velocity fields. Math Comput Simulat 2011;82(4):679–690.
[47] Jiang H. Uniform convergence rates for kernel density estimation. In: Proceedings of the 34th International Conference on Machine Learning - Volume 70, JMLR. org, 2017, p. 1694–1703.
[48] Silverman BW. Density estimation for statistics and data analysis. Chapman and Hall; 1986.
[49] Devroye L, Györfi L. Nonparametric density estimation: L_1 view. Wiley; 1985.
[50] Field Jr RV, Grigoriu M. Convergence properties of polynomial chaos approximations for L_2 random variables. Sandia National Laboratories: No. SAND2007-1262; 2007.